



Second harmonic acoustic responses induced in matter by quasi continuous radiofrequency fields

Stephan Kellnberger, Murad Omar, George Sergiadis, and Vasilis Ntziachristos

Citation: [Applied Physics Letters](#) **103**, 153706 (2013); doi: 10.1063/1.4824709

View online: <http://dx.doi.org/10.1063/1.4824709>

View Table of Contents: <http://scitation.aip.org/content/aip/journal/apl/103/15?ver=pdfcov>

Published by the [AIP Publishing](#)

An advertisement for Integrated Engineering Software. It features a yellow background with a blue and green abstract graphic on the right. The text 'INTEGRATED ENGINEERING SOFTWARE' is in a bold, blue, sans-serif font. Below it, 'Particle and Beam Ray Tracing Simulation' is in a smaller, blue, sans-serif font, followed by 'Send us your model and see LORENTZ in action'. A 'LEARN MORE' button is in a white, sans-serif font with a blue outline. The background has a grid of dotted lines.

INTEGRATED
ENGINEERING SOFTWARE

Particle and Beam Ray Tracing Simulation
Send us your model and see LORENTZ in action

LEARN MORE

Second harmonic acoustic responses induced in matter by quasi continuous radiofrequency fields

Stephan Kellnberger,^{1,a),b)} Murad Omar,^{1,a)} George Sergiadis,² and Vasilis Ntziachristos^{1,b)}

¹*Institute for Biological and Medical Imaging, Technische Universität München and Helmholtz Zentrum München, Ingolstädter Landstraße 1, 85764 Neuherberg, Germany*

²*Department of Electrical and Computer Engineering, Aristotle University, 54124 Thessaloniki, Greece*

(Received 29 July 2013; accepted 25 September 2013; published online 11 October 2013)

We subjected conductive matter and tissue to intermittent continuous-wave radiofrequency fields and investigated whether acoustic responses could be recorded. By placing samples in the near-field of the excitation, we observed frequency-domain acoustic responses from tissues responding to CW radiofrequency excitation. Frequency analysis revealed the generation of 2nd harmonic mechanical waves. This discovery of non-linear responses can lead to alternative measurement concepts of CW radiofrequency deposition in matter and tissues. We offer the theoretical mainframe and discuss sensing applications involving the direct measurement of second harmonic responses representative of CW RF energy deposition in matter. © 2013 AIP Publishing LLC. [<http://dx.doi.org/10.1063/1.4824709>]

Tissue exposure to sub-microsecond electromagnetic (EM) pulsed energy gives rise to acoustic responses and has in the past allowed the formation of images of biological matter.^{1–5} Radiation pulses in the sub-microsecond range have resulted in resolutions of a few millimeters to several hundred microns.¹ Improved resolution has been granted by our introduction of near-field radiofrequency thermoacoustic (NRT) tomography, which optimizes energy coupling efficiency, allowing the use of pulses that are shorter than 100 ns and therefore enable thermoacoustic imaging at spatial resolution in the order of 100 μm .^{2–4} This work was recently replicated by Lou *et al.*⁶

While thermoacoustic responses have so far been generated using electromagnetic pulses in the 100 MHz–3 GHz carrier frequency ranges, it is unknown whether constant wave radiofrequency can generate measurable mechanical responses following radiofrequency absorption.

In this Letter, we interrogated the mechanical responses of biological tissue exposed to constant wave radiofrequency. So far, only pulsed excitation has been used in thermoacoustic observations.^{1–7} Conductive matter, including copper and tissues, was selected to absorb radiofrequency energy. A particular challenge was that constant wave radiofrequency is always on and interferes with conventional ultrasonic detectors. In pulsed-domain thermoacoustics, RF interference with acoustic detectors is avoided, thanks to the time separation of the excitation and detection operations. Similarly, the laser light employed in CW optoacoustic measurements does not generally interfere with the detectors used.^{8,9}

In order to reliably interrogate the presence of mechanical waves from matter, in response to CW radiofrequency, we instead devised herein the use of quasi-CW RF fields, i.e.,

long narrowband CW stimulation of at least 10 μs duration. This particular CW field pattern allowed for temporal separation of RF interference distortion from received acoustic signals, enabling the experimental detection of mechanical responses induced in solid and soft conductive matter. Using this excitation we recorded ultrasonic waves from matter responding to the absorption of radiofrequency fields. Our recordings showed that the ultrasonic waves follow a non-linear performance, resonating at double the frequency of the excitation radiofrequency field. In this paper, we first describe technological aspects of our quasi-CW method, which allowed for non-linear acoustic waveform generation in solid matter. The subsequent theoretical part delineates the non-linear relationship between RF stimulation and acoustic waveform generation, while finally 2nd harmonic acoustic wave induction is demonstrated in biological samples.

The experimental setup employed is schematically illustrated in Fig. 1(a). Excitation signals were generated using a modified high voltage (HV) –30 kV impulse generator. A similar system was previously employed in our NRT studies to perform high resolution thermoacoustic imaging with nanosecond ultrahigh energy pulses.^{2–4} The RF generator could be operated in two different modes.

- (i) In pulsed mode, the capacitive output of the generator ($C_{out} = 1700$ pF) was terminated with custom-built solenoids (coil #1: #turns: 8, diameter: 66 mm, length: 80 mm, inductance: $L_1 = 3.44$ μH ; coil #2: #turns: 7, diameter: 50 mm, length: 80 mm, inductance: $L_2 = 1.51$ μH) in combination with a damping element R , creating an almost critically damped RLC system. Thus, a bipolar excitation profile is generated with a duration of ~ 80 ns as shown in Fig. 1(b).
- (ii) In quasi-CW mode, the output of the generator consisted of the capacitor C_{out} and the inductances L_1/L_2 solely, creating two distinct resonance frequencies ($f_1 = 2.1$ MHz, $f_2 = 3.1$ MHz), which advantageously matched the detection bandwidth of the ultrasonic PZT

^{a)}Stephan Kellnberger and Murad Omar contributed equally to this work.

^{b)}Authors to whom correspondence should be addressed. Electronic addresses: v.ntziachristos@tum.de and stephan.kellnberger@tum.de

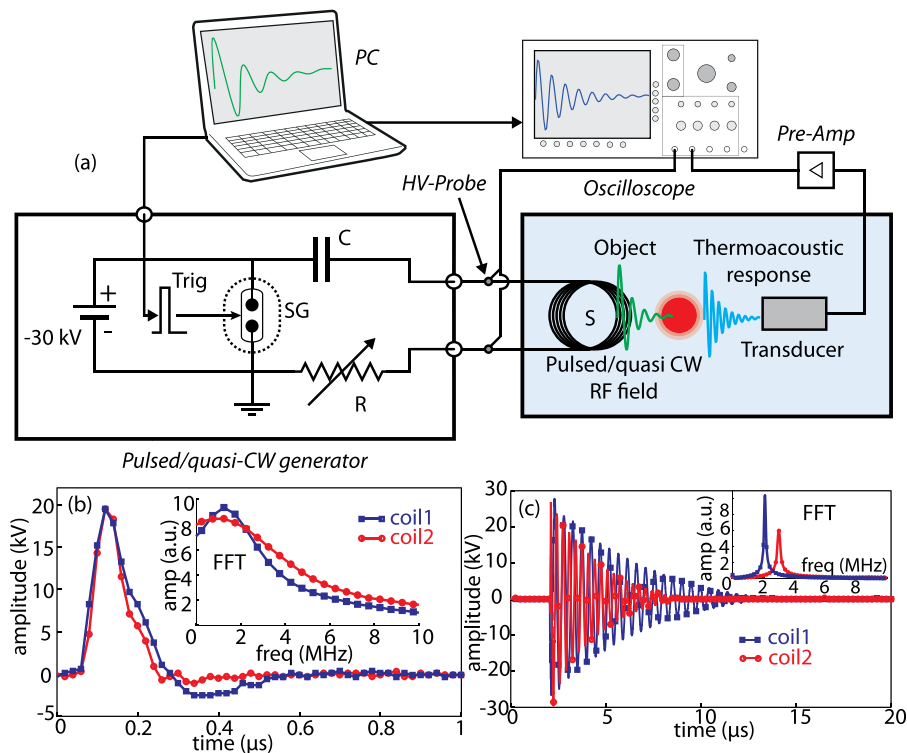


FIG. 1. (a) Schematic representation of the experimental setup. RF excitation is provided by a dedicated pulsed/quasi-CW generator (HV-Probe: High Voltage Probe, Trig: Trigger signal, SG: Spark gap, C: energy storage capacitor, S: solenoid, R: Resistor), (b) Pulsed RF excitation profiles generated by damped coil #1 and coil #2. Inset shows Fourier transformations of the signals, revealing broadband characteristics of the time domain signals, (c) Quasi-CW stimulation produced by coil #1 and coil #2. The narrowband profile of both signals is showcased in the FFT inset.

transducer (lead zirconate titanate; central frequency: $f_c = 3.5$ MHz, bandwidth 76%). The corresponding quasi-CW field profiles are showcased in Fig. 1(c), revealing the time-intermittent characteristics with a time duration of ~ 10 μ s and furthermore the sharp resonance frequency depending on the LC circuit.

Our previous publications on near-field radiofrequency thermoacoustic imaging demonstrated that most of the power (>50%) is dissipated within the close vicinity of the energy transmitting elements,² while electric field distortions caused by conducting objects can be neglected.³ Relying on the increased absorption performance of the near-field and to achieve high RF energy coupling in pulsed and quasi-CW mode, we placed objects in the near-field of the energy coupling solenoids, a geometrical arrangement which is also loosely modeled to mimic conditions of cellular phone energy coupling to human head.

Similar to time domain pulsed thermoacoustic imaging, we first examined whether broadband thermoacoustic responses could be induced in highly dissipative material consisting of a thin copper wire. Copper exhibits significant RF energy absorption due to its high conductivity, resulting in strong acoustic responses that are proportional to the rate of dissipation losses $Q_{RF}(\vec{r}, t) = \sigma(\vec{r})|E(\vec{r}, t)|^2$, where σ relates to the conductivity and E is the electric field amplitude (at frequencies $f < 1$ GHz). Figure 1(b) depicts the broadband excitation profile produced by the RLC impulse generator, measured at the output by means of a high voltage probe. The sub-microsecond pulses exhibited a total energy of 340 mJ, exciting a frequency band below 10 MHz (see Fig. 1(b)). Figure 2 correspondingly depicts the thermoacoustic signal of copper wire, captured by the ultrasound detector when excited by coil #1 (see Fig. 1(b)). Although we applied electromagnetic shielding to the sensor, the strong

high-voltage impulse saturates the detection for a time period of ~ 5 μ s, compromising acoustic signal detection within this time frame. The broadband thermoacoustic response exhibited a signal to noise ratio (SNR) of 29.3 dB and was measured at time point $t = 22$ μ s, corresponding to the position of the copper wire ($d = 33$ mm) from the sensor.

Changing the generator to quasi-CW mode (ii) and exposing the highly dissipative copper wire to quasi-CW RF fields, we observed a significant RF distortion of our acoustic sensor as shown in Fig. 3. During the time period of the quasi-CW profile, the transducer signal was significantly distorted, disabling thermoacoustic wave detection for 18 μ s. However, by placing objects at distances farther than the point of transducer relaxation ($d = 27$ mm), we could separate thermoacoustic waves from RF interferences.

To confirm the detection of frequency domain thermoacoustic signals, we placed a copper wire ($\varnothing = 230$ μ m, length ~ 10 cm, conductivity $\sigma = 5.96 \times 10^7$ S m⁻¹) in close vicinity

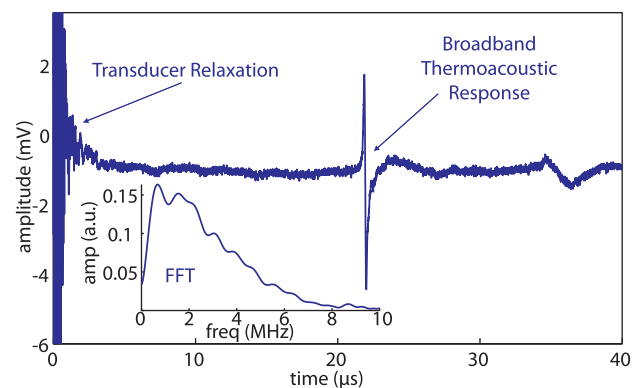


FIG. 2. Broadband thermoacoustic signal acquired by the ultrasound sensor, depicting transducer saturation due to high voltage stimulation. Inset describes the Fourier transform of the filtered thermoacoustic response.

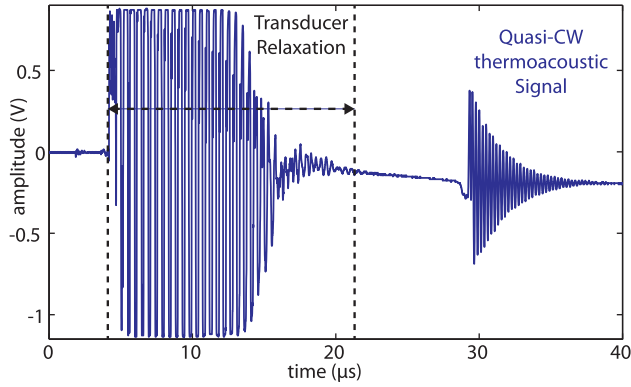


FIG. 3. Signal recorded by transducer when exposing objects to quasi-CW profiles, showing saturation effects corresponding to the duration of the quasi-CW waveform.

of solenoid #1 at a distance of $d = 43.5$ mm from the PZT transducer. Figure 4(a) depicts the quasi-CW stimulation profile along with the RF-interference filtered non-linear thermoacoustic response, induced at time point $t = 29$ μ s, accurately corresponding to the distance of the object from the detector. As observed in the Fourier transform of both RF and acoustic signals, shown in the inset of Fig. 4(a), the acoustic waveform exhibits a clear resonance at double the frequency of the quasi-CW resonance, i.e., $f_{TAS,1} = 2f_1 = 4.2$ MHz. The signal to noise ratio was computed to SNR of 60 dB after 200 averages and 65 dB amplification by a low noise amplifier.

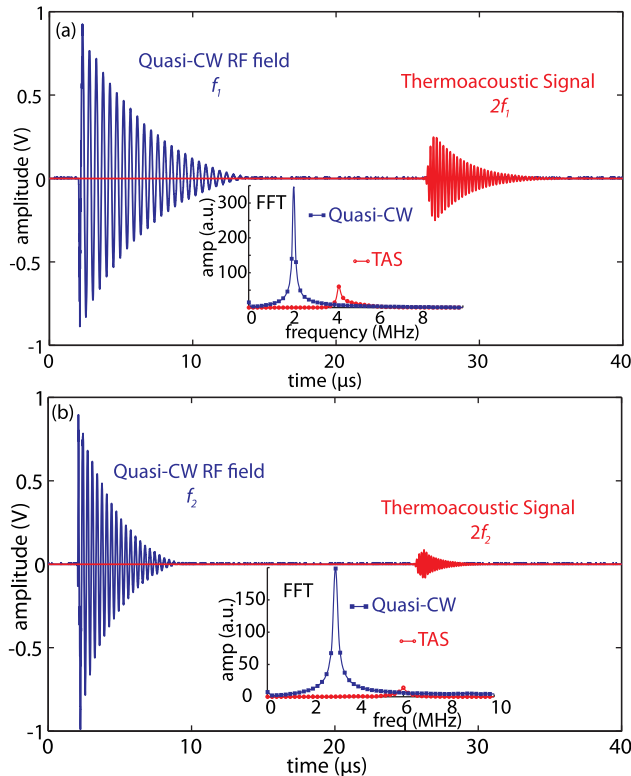


FIG. 4. Quasi-CW thermoacoustic measurements of copper wires at different excitation frequencies. (a) Normalized quasi-CW field $f_1 = 2.1$ MHz and corresponding 2nd harmonic thermoacoustic response (RF interferences are filtered). Inset shows Fourier transformations of RF stimulation and acoustic signals. (b) Quasi-CW stimulation $f_2 = 3.1$ MHz and filtered 2nd harmonic acoustic signal with corresponding Fourier transformations displayed in the inset.

Repeating the measurement at a different carrier frequency $f_2 = 3.1$ MHz using solenoid #2, we could verify a non-linear thermoacoustic response at $f_{TAS,2} = 2f_2 = 6.2$ MHz generated at time point $t = 25.5$ μ s, corresponding to the position of the wire relatively to the transducer. The corresponding waveforms in time and frequency domain are represented in Fig. 4(b), revealing a SNR of 53.7 dB after 65 dB amplification and averaging 200 waveforms. In this case, SNR is lower due to the reduced gain of the transducer above its cut off frequency $f_{cut-off} = 5$ MHz.

The generation of second harmonic acoustic responses from radiofrequency fields is in stark difference to frequency domain optoacoustics using CW modulated light. To understand the underlying phenomena of non-linear acoustic wave induction following the absorption of RF energy, we consider the general photoacoustic wave equation in frequency domain

$$\left(\nabla^2 + \frac{\omega^2}{v_s^2}\right)\hat{p}_x(\vec{r}, \omega) = -j\omega\frac{\beta}{C_p}\left(q\nabla^2\hat{T}(\vec{r}, \omega) + \hat{Q}_x(\vec{r}, \omega)\right), \quad (1)$$

which relates the detected pressure \hat{p}_x to the heating function \hat{Q}_x , whereby β is the thermal coefficient of volumetric expansion, C_p is the specific heat capacity, q is the thermal conductivity, v_s is the speed of sound in water, and T the tissue temperature at position r and time t .

In the case of optical excitation, the heating function can be written as

$$\hat{Q}_{opt}(\vec{r}, \omega) = \mu_a I(\vec{r})\hat{M}(\omega)\eta_{eff}\exp(-\mu_a|z - z_0|), \quad (2)$$

whereby μ_a is the optical absorption coefficient, η_{eff} is the conversion efficiency, I the intensity at position r , and $\hat{M}(\omega)$ relates to the Fourier transform of the modulation term.⁹

Assuming a cosine modulation of laser intensity at frequency f , the time domain–frequency domain relationship

$$m(t) = \cos(2\pi ft) = \cos(\omega_0 t) \xrightarrow{FD} \quad (3)$$

$$\hat{M}(\omega) = \pi[\delta(\omega + \omega_0) + \delta(\omega - \omega_0)]$$

substituted in Eq. (2) yields a linear correlation between optically induced pressure \hat{p}_{opt} and optical power term \hat{Q}_{opt} as a function of ω_0 .

Conversely, RF excitation of tissue can be aptly described by the deposited power function according to Poynting's theorem, i.e.,

$$\hat{Q}_{RF}(\vec{r}, \omega) = \sigma(\vec{r})|\hat{E}(\vec{r}, \omega)|^2 + \pi f \varepsilon''(\vec{r})|\hat{E}(\vec{r}, \omega)|^2 + \pi f \mu''(\vec{r})|\hat{H}(\vec{r}, \omega)|^2, \quad (4)$$

where ε'' and μ'' denote the imaginary part of the complex permittivity and permeability, respectively, \hat{E} is the spectral electric field amplitude, and \hat{H} is the spectral magnetic field amplitude. The wavelengths of the quasi-CW RF fields significantly exceed the sample size; therefore, we approximate a homogeneous field distribution within the sample volume.⁴ Assuming further an electric field $E(\vec{r}, t) = E_0\vec{e}_r \cos(\omega_0 t)$ oscillating at frequency ω_0 , we can rewrite the power of the electric field in the Fourier domain as

$$|\hat{E}(\vec{r}, \omega)|^2 = \frac{\pi}{2} E_0^2 \vec{e}_r [\delta(\omega - 2\omega_0) + \delta(\omega + 2\omega_0) + 2\delta(\omega)]. \quad (5)$$

Equation (5) substituted in Eq. (4) correspondingly yields the non-linear proportionality of RF-induced acoustic pressure \hat{p}_{RF} to the power dissipation \hat{Q}_{RF} as a function of $2\omega_0$.

To examine whether second harmonic responses could also be detected from biological tissues we placed excised pork muscle tissue (size: 4.5 mm × 4.5 mm × 10 mm) at a distance $d = 43.5$ mm from the detector. Similar to time domain thermoacoustic imaging conditions using broadband stimulation, we chose muscle tissue in our quasi-CW experiment due to its relatively high conductivity ($\sigma = 0.5$ S m⁻¹ at 5 MHz) compared to other soft tissues such as liver ($\sigma = 0.3$ S m⁻¹ at 5 MHz) or adipose tissue ($\sigma = 0.015$ S m⁻¹ at 5 MHz).¹⁰ Figure 5 shows the quasi-CW excitation signal at $f_1 = 2.1$ MHz, measured with a high voltage probe and the corresponding thermoacoustic response at $f_{TAS, bio} = 4.2$ MHz. The ultrasonic response was confirmed over a time interval of ~ 10 μ s, corresponding to the excitation duration. Compared to the copper measurement, the signal intensity decreased significantly due to the lower conductivity of biological tissue, resulting in an SNR of 32.2 dB after averaging 200 waveforms and amplification with 65 dB.

The findings herein verify the previously undocumented presence of measurable second harmonic acoustic responses from tissues when placed within quasi-CW radiofrequency fields. In this study, we employed low frequent high energy RF excitation at 2.1 MHz and 3.1 MHz, which enable deep penetration in tissue; however, the physical phenomenon of non-linear acoustic wave induction is not limited to low frequencies but can also be applied at high frequencies in the hundreds of MHz and GHz band limited only by the detection bandwidth of ultrasound sensors. We further offered the theoretical background for the generation of these signals. Measurements of second harmonic acoustic responses correspond to a direct measurement of continuous wave electromagnetic energy absorption by matter such as tissue. Their measurement can be therefore used to quantify RF energy absorption by tissue. Although time-separation was employed herein to offer reliable signal detection, the recent emergence of highly sensitive optical interferometry detectors could enable measurements also of non-intermittent fields.¹¹ Due to the dependence of ultrasonic frequency and depth, we note that this utilization is sensitive to the frequency of the radiofrequency wave employed and the measurement depth achieved.

Second, non-linear acoustic responses could be employed for image generation, in analogy to frequency-domain optoacoustic methods. Since quasi-CW stimulation uses dominating electric fields at low frequencies in the MHz region, imaging contrast will be provided by tissues with different conductivities. Our experiments with quasi-CW excitation profiles were performed within the near-field of

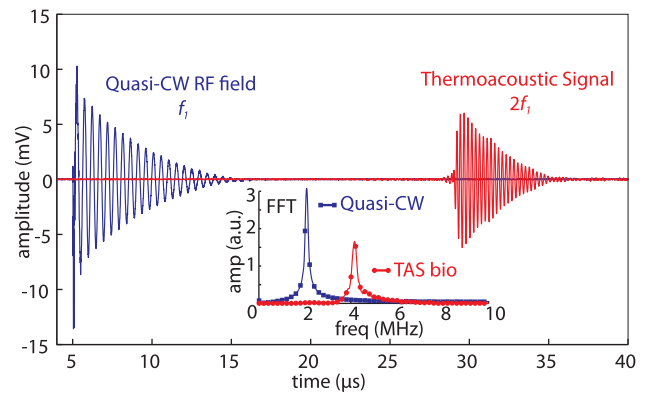


FIG. 5. Quasi-CW stimulation at $f_1 = 2.1$ MHz and RF-filtered 2nd harmonic thermoacoustic response of soft tissue. The FFT of both the excitation and the non-linear acoustic response are represented in the inset.

energy couplers (i.e., solenoids), an arrangement which resembles conditions of cell-phone energy absorption by human tissues such as the brain as the herein employed power of $P_{ave} = 3.4$ W only exceeded the power of cell phones by a factor of 1.4 in average. 2nd harmonic detection of thermoelastic responses could be therefore employed to experimentally measure energy deposition in tissues, in contrast to today's standard, which is based on complex simulations employing numerical algorithms or the specific absorption rate (SAR), which defines the absorption of EM power per volume.¹² While this research investigates the proof of non-linear acoustic responses from tissues, future work will focus on characterizing the 2nd harmonic acoustic responses of various tissue constituents as a function of intensity and frequency. We conclude that 2nd harmonic thermoacoustic measurements can play a measurement role in RF dosimetry and interaction with solid and soft tissues.

V. Ntziachristos acknowledges financial support from the DFG Reinhart-Koselleck-Projekt.

- ¹R. A. Kruger, K. D. Miller, H. E. Reynolds, W. L. Kiser, Jr., D. R. Reinecke, and G. A. Kruger, *Radiology* **216**, 279–283 (2000).
- ²D. Razansky, S. Kellnberger, and V. Ntziachristos, *Med. Phys.* **37**, 4602–4607 (2010).
- ³S. Kellnberger, A. Hajiaboli, D. Razansky, and V. Ntziachristos, *Phys. Med. Biol.* **56**, 3433–3444 (2011).
- ⁴M. Omar, S. Kellnberger, G. Sergiadis, D. Razansky, and V. Ntziachristos, *Med. Phys.* **39**, 4460–4466 (2012).
- ⁵Y. Xu and L. V. Wang, *IEEE Trans. Ultrason. Ferroelectr. Freq. Control* **53**, 542–548 (2006).
- ⁶C. Lou, S. Yang, Z. Ji, Q. Chen, and D. Xing, *Phys. Rev. Lett.* **109**, 218101 (2012).
- ⁷A. Mashal, J. H. Booske, and S. C. Hagness, *Phys. Med. Biol.* **54**, 641–650 (2009).
- ⁸S. Kellnberger, N. Delioliannis, D. Queirós, G. Sergiadis, and V. Ntziachristos, *Opt. Lett.* **37**, 3423–3425 (2012).
- ⁹S. Telenkov and A. Mandelis, *Rev. Sci. Instrum.* **81**, 124901-1-7 (2010).
- ¹⁰S. Gabriel, R. W. Lau, and C. Gabriel, *Phys. Med. Biol.* **41**, 2251–2269 (1996).
- ¹¹A. Rosenthal, D. Razansky, and V. Ntziachristos, *Opt. Lett.* **36**, 1833–1835 (2011).
- ¹²D. Razansky, D. F. Soldea, and P. D. Einziger, *IEEE Trans. Electromagn. Compat.* **47**, 61–67 (2005).